P. R. Bargo, S. A. Prahl, S. L. Jacques, “Collection efficiency of a single optical fiber in turbid media for reflectance spectroscopy,” in OSA Biomedical Topical Meetings, pp. 604–606, (2002).

Collection efficiency of a single optical fiber in turbid media for reflectance spectroscopy

Paulo R. Bargo, Scott A. Prahl and Steven L. Jacques
Oregon Medical Laser Center, Providence St. Vincent Hospital, 9205 SW Barnes Rd,. Portland, OR
OGI School of Science and Engineering, Oregon Health and Science University, 20000 NW Walker Rd., Beaverton, OR 97006
(503) 216-4093, (503)216-2422, pbargo@ece.ogi.edu, prahl@ece.ogi.edu, sjacques@ece.ogi.edu

Abstract: The effect of optical properties on the optical fiber collection efficiency in turbid media was studied experimentally and modeled by Monte Carlo simulations. An analytic expression was obtained to estimate the collection efficiency.

OCIS codes: (170.3660) Light propagation in tissues; (170.3890); Medical optics instrumentation

1. Introduction

Single optical fibers have been commonly used as light delivering and collection tools for optical diagnosis. Authors have proposed their use to determine tissue optical properties [1], measure chromophore relative concentration [2-4] and monitor drug pharmacokinetics [5]. This paper explores the effect of the tissue optical properties on the optical fiber collection efficiency (*f*) when a single optical fiber is used as light source and detector. The optical fiber collection efficiency is defined as the total number of photons collected by the optical fiber that exit the tissue with an angle less than the fiber acceptance angle (numerical aperture – NA [6]) divided by all the photons collected by the fiber. In other words, *f* is the number of photons that couple to the fiber CORE divided by the number of photons that couple to the fiber CORE and CLAD as stated in eq. 1, and can be determined by Monte Carlo simulations.

$$f = \frac{CORE}{CORE + CLAD} \qquad (1)$$

$$f^* = \frac{CORE}{CORE + CLAD + AIR} \qquad (2)$$

It is difficult to determine *f* experimentally since the light lost in the fiber cladding is difficult to measure accurately. For that reason a different collection efficiency (*f**, eq. 2; defined by Saidi [7]) was determined experimentally to compare experiments to theory. The term AIR is used for all the photons that exit the medium outside the optical fiber. The sum CORE + CLAD + AIR is equal to the total diffuse reflectance exiting the tissue and can be calculated by Monte Carlo simulations [8, 9] or Adding Doubling [9].

2. Materials and Methods

2.1. Acrylamide Gel Optical Phantoms Preparation

A 6x2 matrix of different optical property acrylamide gel phantoms was prepared using Intralipid as scattering element and India ink as absorber. Stock Intralipid-20% was calibrated with the added absorber technique. Stock Intralipid-20% ($\mu_s' \cong 200$ cm^{-1} at 630nm) was mixed with water and stock India ink ($\mu_a \cong 58$ cm^{-1} at 630nm) in appropiate proportions. Solutions had absorption coefficients (μ_a) of 0.01, 0.1, 0.5, 1, 5 and 10 cm^{-1} and reduced scattering coefficients (μ_s') of 10 and 20 cm^{-1} at 630nm with a final volume of 40ml. Gels were prepared by adding 8g of acrylamide gel crystals, 0.16g of BIS-acrylamide, 0.100g of amonium persulphate and 0.2ml of TEMED to the solutions while stirring at 38°C. Samples gelled after approximate 2 minutes. Final sample volume was 48ml and samples were assumed to be a semi-infinite homogeneous medium for the purpose of modeling.

2.2. Monte Carlo Simulations

Monte Carlo simulations [8, 9] were performed for the same set of optical properties to establish *f*. Photons were randomly launched within the radius of the fiber forming a collimated beam into a homogenous semi-infinite medium. Henyey-Greenstein phase functions were used to randomly assign propagation angles (θ). The average cosine (or anisotropy, g) was fixed to a typical tissue value of 0.9. Photons were tracked until totally absorbed or until crossing the air/medium boundary. The roulette method [8, 9] was used to conserve energy. Photons that crossed the boundary were summed into three different bins according to the exit location at the surface and the exiting propagation angle (outside fiber = AIR, inside the fiber = CORE, for $\theta <$ NA and = CLAD for $\theta >$ than NA).

2.3. Single fiber Reflectance Measurements

Samples were measured with a single 600μm optical fiber (Tefzel, Ceramoptec) coupled to a bifurcated optical bundle through a SMA adapter. The bifurcated bundle was composed of two 300μm optical fibers (Tefzel,

Ceramoptec) coupled to a single 600µm SMA connector at the distal end and two 300µm SMA connectors at the proximal ends. One fiber was connected to a tungsten-halogen white lamp (Ocean Optics) and the other to a spectrometer (Ocean Optics) controlled by a laptop computer. The setup of the system is shown in figure 1. Acquisition time was set to 30ms and a filter (2OD) was used with all samples and a stronger filter (3OD) was used with a mirror as a sample. The 600µm fiber was placed in contact with the samples with a water drop to avoid the fiber/air/gel refractive index mismatch.

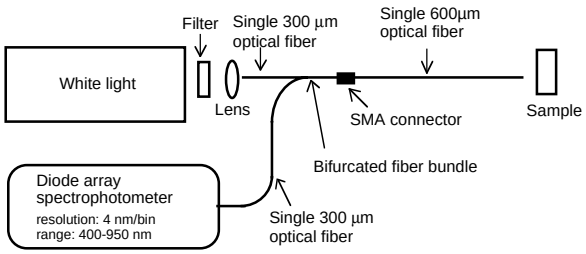

Fig. 1. Experimental setup. Acquisition time was set to 30ms and filters were placed before coupling to optical fiber.

f^*_{sample} was determined by normalizing the sample measurement by a measurement (M_{mirror}) of a mirror (R_{mirror}=0.90) to cancel the effects of source (S) and detector (D) spectral response as shown in equations 3 and 4:

$$\frac{M_{sample}}{M_{mirror}} = \frac{S \cdot R_{sample} \cdot f^*_{sample} \cdot D}{S \cdot R_{mirror} \cdot f^*_{mirror} \cdot D} = \frac{R_{sample} \cdot f^*_{sample}}{R_{mirror} \cdot 1} \quad (3)$$

$$f^*_{sample} = \frac{M_{sample} \cdot 0.90}{M_{mirror} \cdot R_{sample}} \quad (4)$$

f^*_{mirror} was assumed to be 1 since all the light that hits the mirror returns to the fiber with an angle smaller than the acceptance angle. R_{sample} (total diffuse reflectance) was obtained by a forward Adding Doubling calculation [8] with knowledge of the sample optical properties.

3. Results

Figure 2 shows the results for f^* determined by Monte Carlo (empty symbols) and experiments (filled symbols) for two μ_s' (□ = 10cm^{-1}, and ◊ = 20 cm^{-1}) and six μ_a (greater μ_a to the left). f^* is plotted as a function of X[-] defined as $X = \delta \bullet mfp'/d^2$, where $\delta = (3\,\mu_a(\mu_a + \mu_s'))^{-1/2}$, $mfp' = 1/(\mu_a + \mu_s')$ and d is the diameter of the optical fiber.

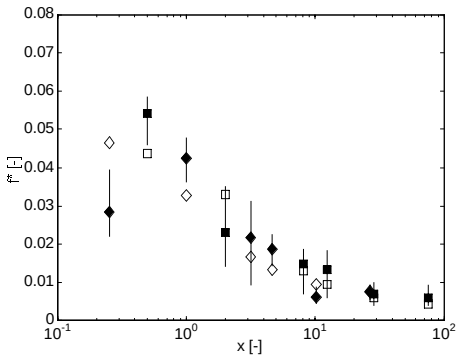

Fig. 2. f^* from Monte Carlo (empty symbols) and experiment (filled symbols). See text for details.

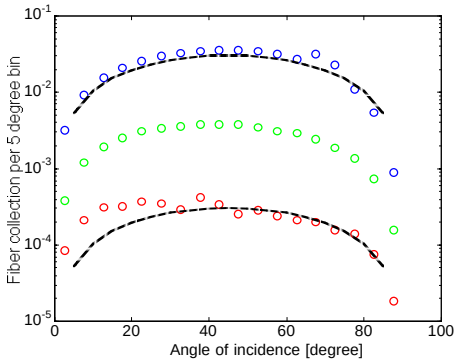

Fig. 3. Collection efficiency f per 5° bin. Integration of these values from 0 to the NA equals f for that NA.

Figure 3 demonstrates the dependence of the collection efficiency on the optical properties by plotting f as a function of collection angle bin (three μ_s' 80, 20 and 1 cm^{-1}, top to bottom). In the same figure plots of COS(θ)SIN(θ) (dashed lines; see eq. 5) show the similarities of the data to this simple expression for higher scattering and the differences for low scattering.

Monte Carlo simulations for a fiber diameter of 600µm and NA of 0.39 immersed in a medium with index of refraction of 1.35 (equivalent to a half angle of $\sin^{-1}(0.39/1.35) = 16.79^o$) is showed in figure 4. A side view of the 3D plot shows that for μ_s' above 20 cm^{-1} f approaches a value of 0.0835.

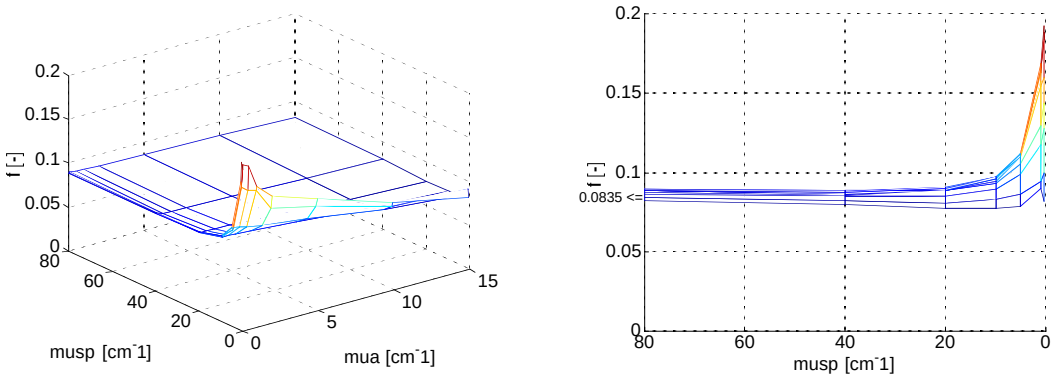

Fig. 4. (LEFT) 3D plot of *f* as a function of optical properties (RIGHT) side view of 3D plot. Graphs are for a 600μm optical fiber with NA = 0.39 and index of refraction of the medium = 1.35.

4. Discussion

Comparison between Monte Carlo (empty symbols) and experimental (filled symbols) *f** in figure 2 show good agreement for physiologically relevant μ_s'. Larger errors were observed for higher absorption (left-most points) probably due to the reduced signal/noise ratio for those measurements. Data tends to collapse to a monotonic sigmoidal curve when plotted against the non-dimensional parameter X in a semi-log plot.

Equation 1 can also be interpreted as the total fraction of light that reaches the optical fiber with an angle smaller than that defined by the NA (θ_1) divided by the total light that couples to the fiber at all angles, as stated in eq.5. Integration of eq.5 in spherical coordinates shows that *f* should be equal to $\sin^2(\theta_1)$.

$$f = \frac{\int_0^{2\pi} d\phi \int_0^{\theta_1} \cos(\theta)\sin(\theta)d\theta}{\int_0^{2\pi} d\phi \int_0^{\frac{\pi}{2}} \cos(\theta)\sin(\theta)d\theta} = \frac{\pi \sin^2(\theta)\Big|_0^{\theta_1}}{\pi \sin^2(\theta)\Big|_0^{\frac{\pi}{2}}} = \sin^2(\theta_1) \qquad (5)$$

For a NA of 0.39 and a medium with index of refraction of 1.35, θ_1 is equal to 16.79°. Applying this angle in equation 5 gives $f = 0.0835$. The value of *f* calculated from equation 5 is a good first approximation for most optical properties, as shown in figure 4. But it does not agree for small (physiologically relevant) values of μ_s' (figure 4 RIGHT). The cone of collection of an optical fiber (defined by the fiber NA) is dependent only on the indices of refraction of the fiber core/clad and the medium where the fiber is immersed [6]. Changes in the optical fiber collection efficiency for turbid media arises from differences in the angular distribution of the photons that reach the fiber for different optical properties, as observed in figure 3 for low scattering (bottom curve). These changes are not caused by an intrinsic parameter of the optical fiber but arise from its use in a turbid media, like biological tissues. The parameter *f* can be used as a practical guide for choosing the NA of an optical fiber for biomedical applications.

5. References

1. T. P. Moffitt and S. A. Prahl, "Sized-fiber reflectometry for measuring local optical properties", IEEE JSTQE, accepted for publication, (2001).
2. S.L.Jacques, "Reflectance spectroscopy with optical fiber devices and transcutaneous bilirubinometers" in Biomedical Optical Instrumentation and Laser-Assisted Biotechnology", 83-94, A.M. Verga Scheggi et al, Ed.(Kluwer Academic Publishers, Netherlands, 1996)
3. B.W. Pogue and G. Burke, "Fiber-optic bundle design for quantitative fluorescence measurement from tissue", Appl.Opt., **37** (31), 7429-7436 (1998).
4. D.R. Braichotte, J.F.Savary, P. Monnier and H.E. van den Bergh, "Optimizing Light dosimetry in photodynamic therapy of early stage carcinomas of esophagus using fluorescence spectroscopy", Laser Surg. Med., **19**, 340-346 (1996).
5. D.R Braichotte, G.A. Wagnieres, R. Bays, P. Monnier and H.E van den Bergh, "Clinical pharmacokinetic studies of photofrin by fluorescence spectroscopy in the oral cavity, the esophagus and the bronchi", Cancer, **75** (11), 2768-2778 (1995).
6. J. Wilson and J.F.B.Hawkes, "Optoelectronics: An Introduction", 2nd Edition, Prentice Hall (1989).
7. L.S. Saidi, "Transcutaneous optical measurement of hyperbilirubinemia in neonates", PhD dissertation, Rice University, Houston, Texas, USA (1992)
8. L. Wang, S.L. Jacques and L. Zheng "MCML – Monte Carlo modeling of light transport in multi-layered tissues", Comp. Meth.Prog. in Biomed **47**, 131-146 (1995).
9. S.A Prahl, "Light Transport in Tissue", PhD dissertation, University of Texas, Austin, Texas, USA (1988).